

Molecular motion and disorder in trimethyloxosulphonium fluoroborate

This article has been downloaded from IOPscience. Please scroll down to see the full text article.

1992 J. Phys.: Condens. Matter 4 5433

(<http://iopscience.iop.org/0953-8984/4/24/013>)

View [the table of contents for this issue](#), or go to the [journal homepage](#) for more

Download details:

IP Address: 171.66.16.159

The article was downloaded on 12/05/2010 at 12:08

Please note that [terms and conditions apply](#).

Molecular motion and disorder in trimethyloxosulphonium fluoroborate

E C Reynhardt, S Jurga† and K Jurga†

Department of Physics, University of South Africa, PO Box 392, Pretoria 0001, South Africa

Received 28 January 1992, in final form 30 March 1992

Abstract. Proton and fluorine second moments and spin–lattice relaxation times have been measured in a polycrystalline sample of trimethyloxosulphonium fluoroborate. Methyl groups execute threefold reorientation with an activation energy of 9.2 ± 0.5 kJ mol⁻¹. The activation energy for the threefold reorientation of the anion is 33 ± 2 kJ mol⁻¹. The disorder of the BF₄⁻ ion is dynamic. The ion jumps between two equilibrium orientations which have six fluorine and two boron equilibrium positions. The activation energy for this rotational–translational motion is 8.8 ± 0.5 kJ mol⁻¹. Further reorientations of the ion about its symmetry axes result in an isotropically reorienting ion. The activation energy for this motion is 17.6 ± 0.8 kJ mol⁻¹.

1. Introduction

Trimethyloxosulphonium fluoroborate (TMOSFB), (CH₃)₃SOBF₄, is an interesting compound from an NMR point of view. The two ions, (CH₃)₃SO⁺ and BF₄⁻ are approximately globular in shape and it is therefore expected that a variety of molecular motions should be identifiable. Apart from the methyl reorientations, the entire TMOS ion can reorient about the threefold axis which coincides with the O–S bond. At higher temperatures an isotropic reorientation of this ion about its centre of mass is possible. In LiBF₄ Reynhardt and Lourens (1984) found that the BF₄⁻ ion diffuses through the lattice above 385 K, while a theoretical study of the geometry of an isolated LiBF₄ molecule (Zakzhevskii *et al* 1980) identified three possible configurations of the molecule with the energy difference between the bidentate and tridentate configurations low enough (~ 12 kJ mol⁻¹) to allow oscillation between the two configurations. The molecular dynamics of trimethyloxosulphonium halides (F, Cl, Br and I) were discussed by Jurga *et al* (1981). It was found that the activation energies for threefold reorientations of methyl groups and the TMOS ion decrease with increasing anion size. An x-ray crystal structure determination of TMOSFB (Zimmermann *et al* 1963) revealed that the space group is *Pbcn* with $z = 8$. Although the TMOS ion is not crystallographically required to have any symmetry, its symmetry closely approximates $3m$. The BF₄⁻ ions are crystallographically of two types and are both required to have symmetry 2. However, these ions achieve this symmetry in a statistical (disordered) manner.

† Permanent address: Institute of Physics, A Mickiewicz University, 60–780 Poznan, Poland.

Apart from the identification and description of the reorientations of the TMO⁺ ion, it should be interesting to establish whether the disorder of the BF₄⁻ ion is dynamic and, if so, to try to obtain some information about the reorientation mechanism associated with the disorder.

In this paper we report proton and fluorine second moments and spin-lattice relaxation times in the laboratory frame as a function of temperature in the range $77 < T < 360$ K. The interpretation of the results sheds some light on the dynamical disorder of the lattice.

2. Experimental details

2.1. Sample preparation

Crystals of TMO⁺ were prepared according to the method described by Smith (1959). A sample of the powdered compound was sealed in a pyrex tube after it had been evacuated for several hours.

2.2. Second moments

Experimental ¹H and ¹⁹F second moments, $M_2(\text{H})$ and $M_2(\text{F})$, were obtained as a function of temperature by using a homemade continuous wave spectrometer operating at 28 MHz and integrating numerically the first derivatives of the absorption line. Corrections for finite modulation amplitudes were made.

The temperature was varied and regulated by a conventional nitrogen gas flow system.

2.3. Spin-lattice relaxation times

Proton and fluorine spin-lattice relaxation times in the laboratory frame, $T_1(\text{H})$ and $T_1(\text{F})$, were measured at 25 MHz on a homemade pulse spectrometer by employing the saturation and $90^\circ - \tau - 90^\circ$ pulse sequences for long and short relaxation times respectively. The decay of the proton and fluorine magnetizations was non-exponential over a narrow temperature range ($294 > T > 260$ K), while in the vicinity of $\beta = 8 \text{ K}^{-1}$ slight non-exponentiality was observed, but the two relaxation times could not be isolated successfully.

3. Results

3.1. Second moments

The proton second moment, $M_2(\text{H})$, shown in figure 1, exhibits two plateaux in the above-mentioned temperature range, that is $1.9 \pm 0.2 \text{ G}^2$ between 270 K and 360 K and $8.2 \pm 0.3 \text{ G}^2$ between 150 K and 200 K.

The fluorine second moment, $M_2(\text{F})$, also has two plateaux, as shown in figure 1. Above 240 K $M_2(\text{F}) = 1.1 \pm 0.1 \text{ G}^2$, while between 150 K and 200 K it is $1.9 \pm 0.1 \text{ G}^2$.

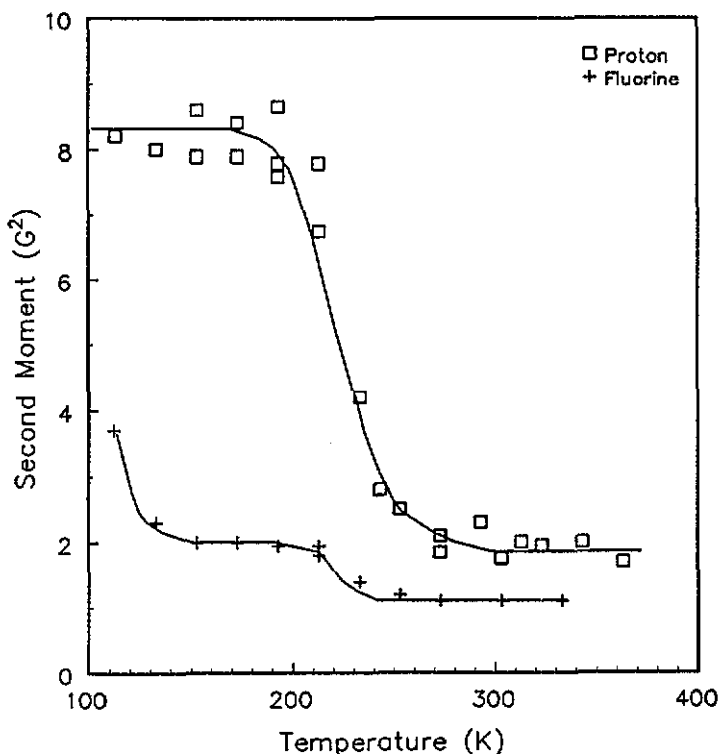


Figure 1. Proton and fluorine second moments as a function of temperature.

3.2. Spin-lattice relaxation times

The proton spin-lattice relaxation time in the laboratory frame, $T_1(\text{H})$, is displayed in figure 2 as a function of $1000/T$ ($= \beta$). $T_1(\text{H})$ shows two minima, with the deeper one (~ 24 ms) occurring at $\beta \simeq 8 \text{ K}^{-1}$ and the shallower one (~ 40 ms) at $\beta \simeq 2.6 \text{ K}^{-1}$.

The fluorine spin-lattice relaxation time in the laboratory frame, $T_1(\text{F})$, is also shown in figure 2 as a function of β . It exhibits three minima, that is at 2.75 K^{-1} (~ 190 ms), 6.8 K^{-1} (~ 26 ms) and 11 K^{-1} (~ 20 ms).

4. Discussion and conclusions

4.1. Disorder of the BF_4 ion

Fluorine and boron equilibrium positions at one of the two BF_4^- sites, in the vicinity of $(0, \frac{1}{2}, \frac{1}{4})$, are shown in figure 3. There are six fluorine and two boron positions. Four of the fluorine positions and both boron positions have occupancy $\frac{1}{2}$, while two fluorine positions have occupancy 1, as shown in the diagram. If this disorder is static, half the sites with occupancy $\frac{1}{2}$ are never occupied. However, if the disorder is dynamic, all these sites are occupied, but only for half of the time. A closer look at figure 3 reveals that a twofold reorientation about an axis parallel to the b axis explains the existence of two boron and six fluorine atomic positions with the relative

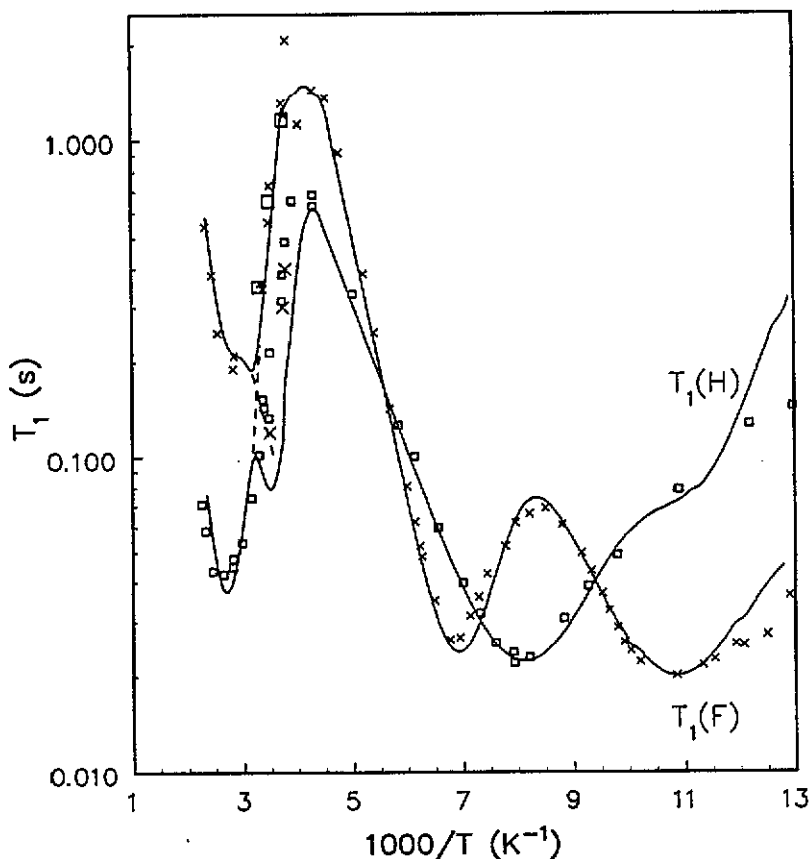


Figure 2. Proton spin-lattice relaxation time as a function of inverse temperature. The lines represent best fits of the theory to the data.

occupancies obtained by x-ray diffraction. The same situation exists at the symmetry related BF_4^- ion in the vicinity of $(\frac{1}{2}, \frac{1}{2}, \frac{1}{4})$.

From figure 3 it is clear the a 180° rotation of the BF_4^- ion about the axis indicated in the figure, moves the ion into a different orientation. Fluorine atoms at sites F1 and F2 interchange positions, but these sites are always occupied, except during the relatively short time when the jump motion takes place. Another fluorine atom jumps between sites F3 and F3', while the fourth fluorine atom jumps between sites F4 and F4'. At the same time the boron atom jumps between two equilibrium positions. This BF_4^- ion motion can be described as a rotational-translational motion. It is also possible that the ion jumps about one or more of its six C_2 and four C_3 axes. A combination of a C_2 reorientation and a reorientation about the twofold axis shown in the figure results in an isotropic reorientation in which each of the F-F internuclear vectors occupies all twelve F-F vector orientations (six for the F1F2F3F4 orientation and six for the F2F1F3'F4' orientation).

4.2. Second moments

The dipolar second moments can be calculated by using the formulae (Van

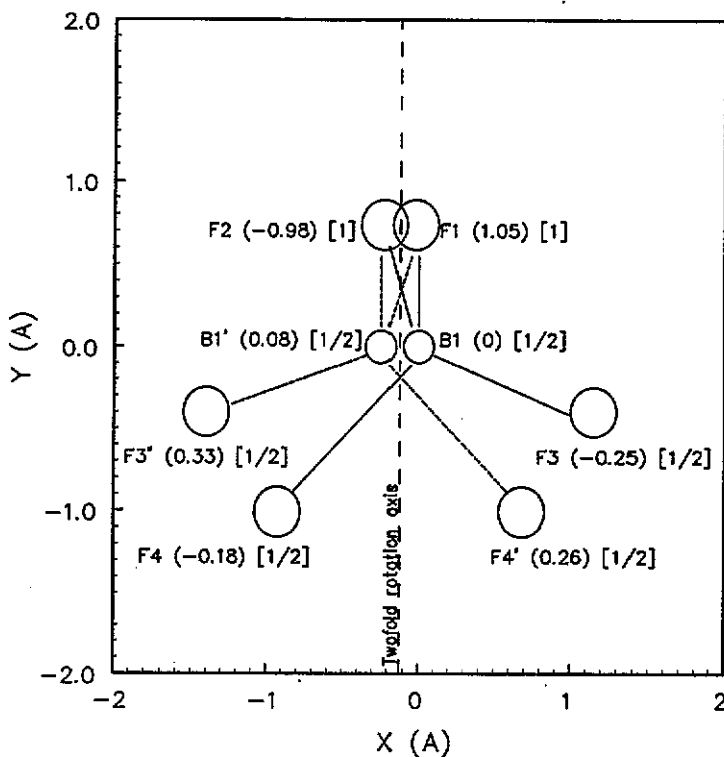


Figure 3. Equilibrium positions of fluorine and boron atoms in the vicinity of $(0, \frac{1}{2}, \frac{1}{4})$ in the unit cell. Numbers between parentheses indicate the z coordinates, while numbers between square brackets denote the occupancies of the sites.

Vleck 1948)

$$M_2(k) = \sum_j M_2(k-j) \quad (1)$$

with

$$M(k-k) = \frac{9}{20} \gamma_k^2 \hbar^2 \sum_l r_{il}^{-6} \quad (2)$$

and

$$M(k-j) = \frac{4}{15} f_j \gamma_j^2 \hbar^2 S_j (S_j + 1) \sum_l r_{il}^{-6}. \quad (3)$$

Here $k = {}^1\text{H}$, ${}^{19}\text{F}$ and $j = {}^{10}\text{B}$, ${}^{11}\text{B}$, ${}^{13}\text{C}$, ${}^{33}\text{S}$, ${}^1\text{H}$ and ${}^{19}\text{F}$, and f_j and S_j are respectively the natural abundance and spin of the isotope with gyromagnetic ratio γ_j . The summations in equations (2) and (3) are over all neighbouring ions (l).

In the presence of a molecular reorientation (Watton *et al* 1970)

$$r_{il}^{-6} = \langle r^{-3} \rangle^2 - 3 \{ \langle x^2/r^5 \rangle \langle y^2/r^5 \rangle + \langle x^2/r^5 \rangle \langle z^2/r^5 \rangle + \langle y^2/r^5 \rangle \langle z^2/r^5 \rangle \\ - \langle xy/r \rangle^2 - \langle xz/r \rangle^2 - \langle yz/r \rangle^2 \} \quad (4)$$

where $r = |\mathbf{r}_{ij}|$. The angular brackets indicate an average over all orientations of the internuclear vector \mathbf{r}_{ij} .

Using these expressions and the atomic coordinates listed by Zimmerman *et al* (1963), after the fluorine coordinates had been adjusted to give more realistic B-F bond distances of 1.43 Å (Sutton 1958), the intramolecular $M_2(\text{F})$ values listed in table 1 were calculated for a stationary ion and for the twofold reorientation of the BF_4^- ion discussed above.

Table 1. Calculated intramolecular ^{19}F second moments.

Motion of BF_4^-	$M_2(\text{F-F})$ (G^2)	$M_2(\text{F-}^{11}\text{B})$ (G^2)	$M_2(^{10}\text{B})$ (G^2)	$M_2(\text{F})$ (G^2)
Stationary	10.0	7.6	0.7	18.3
Twofold reorientation	4.8	3.7	0.3	8.8

Since the proton positions are not known, it is not possible to calculate all the relevant second moment contributions accurately. With a view to obtaining reasonable estimates of these values, all the protons belonging to a methyl group were placed at their centre of mass and intermolecular second moments calculated for various combinations of molecular reorientations of the TMOs and BF_4^- ions. These values are therefore only rough estimates. The intramolecular TMOs contributions were assumed to be the same as the values calculated by Andrew and Canepa (1972) for trimethylammonium chloride. The results are listed in tables 2 and 3.

Table 2. Calculated intramolecular ^1H second moments (Andrew and Canepa 1972).

Motion of TMOs	$M_2(\text{H-H})$ (G^2)
Rigid	25.0
Methyl reorientation	7.5
Triad ionic and methyl reorientation	1.1
IR	0.0

Table 3. Calculated ^1H and ^{19}F second moments.

Motion	$M_2(\text{H-H})$ (G^2)	$M_2(\text{H-F})$ (G^2)	$M_2(\text{H-B})$ (G^2)	$M_2(\text{H})$ (G^2)	$M_2(\text{F-F})$ (G^2)	$M_2(\text{F-H})$ (G^2)	$M_2(\text{F-B})$ (G^2)	$M_2(\text{F})$ (G^2)
R R R	25.9	0.6	0.1	26.6	12.0	2.9	16.0	30.9
C ₃ R R	9.0	0.6	0.1	9.6	12.0	2.9	16.0	30.9
R R C ₂	25.9	0.5	0.1	26.5	6.7	2.9	12.4	22.0
C ₃ R C ₂	9.0	0.5	0.1	9.6	6.7	2.9	12.4	22.0
C ₃ R IR	9.0	0.3	0.1	9.4	0.3	0.9	0.0	1.2
C ₃ C ₃ IR	1.8	0.3	0.1	2.2	0.3	0.9	0.0	1.2
C ₃ IR IR	0.7	0.3	0.1	1.1	0.3	0.9	0.0	1.2

The $M_2(\text{F})$ and $M_2(\text{H})$ plateaux above 270 K of $1.1 \pm 0.1 \text{ G}^2$ and $1.9 \pm 0.2 \text{ G}^2$, respectively, agree well with the calculated values of 1.2 G^2 and 2.2 G^2 for a model with the TMOS ion executes a threefold (C_3) reorientation about the O-S bond and all the methyl groups execute similar reorientations about their S-C bonds, while the BF_4^- ion is involved in an isotropic reorientation (IR) in which each F-F internuclear vector occupies all the available orientations within a time that is short compared with the inverse of the rigid lattice line width.

The plateaux between 150 K and 200 K seem to be in rough agreement with the calculated second moments for a stationary TMOS ion with reorienting methyl groups and a BF_4^- ion that reorients isotropically.

4.3. Spin-lattice relaxation times

4.3.1. *Theory.* Taking into account the dipolar interactions between ^1H , ^{19}F and ^{11}B nuclei only, the time variation of the nuclear magnetizations can be presented in matrix form as (Kozak *et al* 1987)

$$\begin{bmatrix} dM_z(\text{H})/dt \\ dM_z(\text{F})/dt \\ dM_z(\text{B})/dt \end{bmatrix} = \begin{bmatrix} -R_{\text{H}} & -R_{\text{HF}} & -R_{\text{HB}} \\ -R_{\text{FH}} & -R_{\text{F}} & -R_{\text{FB}} \\ -R_{\text{BH}} & -R_{\text{BF}} & -R_{\text{B}} \end{bmatrix} \begin{bmatrix} M_z(\text{H}) - M_0(\text{H}) \\ M_z(\text{F}) - M_0(\text{F}) \\ M_z(\text{B}) - M_0(\text{B}) \end{bmatrix} \quad (5)$$

where $M_z(\text{H})$, $M_z(\text{F})$, $M_z(\text{B})$ and $M_0(\text{H})$, $M_0(\text{F})$, $M_0(\text{B})$ are the z components of the proton, fluorine and ^{11}B nuclear magnetizations at time t and at equilibrium respectively. The quantities R_{H} , R_{F} , R_{B} , R_{HF} , R_{FH} , R_{HB} , etc are the elements of the relaxation matrix. The solutions of these equations are

$$\begin{aligned} & [M_0(k) - M_z(k)] / M_0(k) \\ &= \exp(-\lambda_1 t) \left((R_k - \lambda_2)(R_k - \lambda_3) + \sum_l R_{kl} R_{lk} \right) / (\lambda_1 - \lambda_2)(\lambda_1 - \lambda_3) \\ &+ \exp(-\lambda_2 t) \left((R_k - \lambda_1)(R_k - \lambda_3) + \sum_l R_{kl} R_{lk} \right) / (\lambda_2 - \lambda_1)(\lambda_2 - \lambda_3) \\ &+ \exp(-\lambda_3 t) \left((R_k - \lambda_1)(R_k - \lambda_2) + \sum_l R_{kl} R_{lk} \right) / (\lambda_3 - \lambda_1)(\lambda_3 - \lambda_2) \end{aligned} \quad (6)$$

where λ_1 , λ_2 and λ_3 are the eigenvalues of the relaxation matrix.

In terms of second moment reductions and spectral density functions the matrix elements are given by

$$R_k = \frac{1}{2} \gamma_k^2 \sum_i \sum_j \Delta M_2(k-j)_i g(\omega_{kj}, \tau_i) + \frac{1}{2} \gamma_k^2 \sum_i \Delta M_2(k-k)_i g(\omega_{kk}, \tau_i) \quad (7)$$

$$R_{kl} = \frac{1}{2} \gamma_k^2 \sum_i \Delta M_2(k-l)_i g(\omega_{kl}, \tau_i) \quad (8)$$

where k, j and $l = {}^1\text{H}, {}^{19}\text{F}$ and ${}^{11}\text{B}$. The first summations in equations (7) and (8) are over all reorientation mechanisms. The spectral density functions are given by

$$g(\omega_{kj}, \tau_i) = \tau_i / \left[1 + (\omega_k - \omega_j)^2 \tau_i^2 \right] + 3\tau_i / \left(1 + \omega_k^2 \tau_i^2 \right) + 6\tau_i / \left[1 + (\omega_k + \omega_j)^2 \tau_i^2 \right] \quad (9)$$

$$g(\omega_{kk}, \tau_i) = \frac{4}{3} \left[\tau_i / \left(1 + \omega_k^2 \tau_i^2 \right) + 4\tau_i / \left(1 + 4\omega_k^2 \tau_i^2 \right) \right] \quad (10)$$

and

$$g(\omega_{kl}, \tau_i) = -\tau_i / \left[1 + (\omega_k - \omega_l)^2 \tau_i^2 \right] + 6\tau_i / \left[1 + (\omega_k + \omega_l)^2 \tau_i^2 \right]. \quad (11)$$

4.3.2. Proton spin-lattice relaxation. From the discussion of the second moment results it follows that the $T_1(\text{H})$ minimum at $\beta \simeq 8 \text{ K}^{-1}$ is due to the threefold reorientation of methyl groups, while the minimum at $\beta \simeq 2.6 \text{ K}^{-1}$ reflects the threefold reorientation of the TMOS ion.

Since ${}^{11}\text{B}$ nuclei have spin $\frac{3}{2}$, their relaxation is dominated by the quadrupole interaction and a relatively large quadrupolar term has to be added to equation (7) for $k = {}^{11}\text{B}$. On the other hand, the cross relaxation terms R_{BH} and R_{HB} result only from relatively weak proton-B dipolar interactions. Therefore, $R_{\text{H}}R_{\text{B}} \gg R_{\text{HB}}R_{\text{BH}}$ and the relaxation equations for these nuclei are decoupled. The same arguments are valid in the case of the fluorine and boron spin systems. Therefore, equation (6) is reduced to

$$\begin{aligned} [M_0(k) - M_z(k)] / M_0(k) &= (R_k - \lambda_1) / (\lambda_1 - \lambda_2) \exp(-\lambda_1 t) \\ &+ (R_k - \lambda_1) / (\lambda_2 - \lambda_1) \exp(\lambda_2 t) \end{aligned} \quad (12)$$

with

$$\lambda_{1,2} = \frac{1}{2}(R_{\text{H}} + R_{\text{F}}) \pm \frac{1}{2} \left[(R_{\text{H}} + R_{\text{F}})^2 - 4R_{\text{H}}R_{\text{F}} + 4R_{\text{HF}}R_{\text{FH}} \right]^{1/2} \quad (13)$$

Above about 330 K all terms involving τ_i , where i refers to the motion of the BF_4^- ion, may be neglected since $\omega_{\text{F}}\tau_i \ll \omega_{\text{H}}\tau_{ii}$, where ii refers to the motion of the TMOS ion. Also $\omega_{\text{H}}\tau_{ii}$ terms may be dropped since $\omega_{\text{H}}\tau_{ii} \ll 1$. Finally $\Delta M_2(\text{H-H})$ in the expression for R_{H} (equation (7)) is much larger than the ΔM_2 s in all of the other terms of the relaxation matrix. Therefore, $\lambda_1 \simeq R_{\text{F}}$ and $\lambda_2 \simeq R_{\text{H}}$. Substitution of these values into equation (12) yields exponential decays.

In the temperature region 294–200 K the reorientation of the TMOS ion is slower and $\omega_{\text{H}}\tau_{ii} > 1$. Of the terms in τ_{ii} , those involving $\tau_{\text{H}} / [1 + (\omega_{\text{H}} - \omega_{\text{F}})^2 \tau_{ii}^2]$ predominate and since there is one of these terms in each of the elements of the relaxation matrix, the four elements are approximately of the same order of magnitude. Mutual spin flips of neighbouring protons and fluorine nuclei occur in this region. The rate of this cross relaxation is independent of the spin-lattice relaxation and is the

cause of the non-exponential decays of the proton and fluorine FIDs. In this region $\lambda_2 \simeq R_H \simeq R_F$.

In the region where the C_3 reorientations of methyl groups dominate the proton relaxation rate ($T < 250$ K), the non-exponentiality is not severe and it is therefore assumed that $T_1 \simeq R_H^{-1}$.

A best fit of equations (5) to (13) to the data, shown as full curves in figure 2, yielded the motional parameters listed in table 4. The total $\Delta M_2(H)$ associated with threefold reorientations of all the methyl groups is 17 G^2 (table 3). The second-moment reduction obtained from the best fit to the $T_1(H)$ data is 9 G^2 , which is only 53% of the calculated reduction. It is possible that some of the methyl groups have lower activation energies for this motion and that the $T_1(H)$ minimum associated with their threefold reorientation occurs at temperatures lower than the minimum temperature reached in this experiment.

Table 4. Motional parameters associated with reorientations of the TMS and BF_4^- ions.

Parameter	Methyl C_3	TMS C_3	BF_4^- C_2	BF_4^- isotropic
E (kJ mol $^{-1}$)	9.2 ± 0.5	33 ± 2	8.8 ± 0.5	17.6 ± 0.8
$\log[\tau_0$ (s)]	-12.4 ± 0.1	-13.1 ± 0.1	-13.0 ± 0.1	-14.6 ± 0.1
$M_2(\text{H-H})$ (G^2)	9 ± 1	6 ± 1	0.0	0.0
$M_2(\text{H-F})$ (G^2)	1.0 ± 0.2	0.1 ± 0.2	0.3 ± 0.2	0.2 ± 0.1
$M_2(\text{H-B})$ (G^2)	0.0	0.0	0.0	0.0
$M_2(\text{F-F})$ (G^2)	0.0	0.0	5.2 ± 0.3	4.8 ± 0.3
$M_2(\text{F-H})$ (G^2)	0.7 ± 0.2	0.6 ± 0.2	1.5 ± 0.3	0.7 ± 0.3
$M_2(\text{F-B})$ (G^2)	0.0	0.0	3.9 ± 0.3	3.7 ± 0.3

From tables 3 and 4 it can be seen that the calculated and experimentally obtained second moment reductions are in reasonable agreement.

4.3.3. Fluorine spin-lattice relaxation. It is assumed that the low-temperature $T_1(F)$ minimum is due to the reorientation of the BF_4^- ion about the axis indicated in figure 3 and that the second $T_1(F)$ minimum reflects an additional motion of the same ion. The high temperature $T_1(F)$ minimum coincides with a $T_1(H)$ minimum, which is due to the threefold reorientation of the TMS ion. It is clear that this minimum is due to the modulation of the intermolecular dipolar interactions between the TMS and BF_4^- ions, as already discussed in the previous section.

It is expected that the relaxation should be non-exponential on the low-temperature sides of the low-temperature $T_1(F)$ minima for the same reasons given in the case of the high-temperature $T_1(H)$ and $T_1(F)$ minima. However, although non-exponentiality was observed in these regions, it was less prominent than in the high-temperature region. The results are therefore interpreted by fitting equation (7) to the data and ignoring the non-exponential behaviour.

The curves in figure 2 represent best fits of equations (7) to the experimental data. From tables 3 and 4 it is clear that the calculated second-moment reductions and the corresponding values obtained from the fits to the $T_1(F)$ data are in good agreement.

Acknowledgments

The Foundation for Research and Development and the Research and Bursaries

Committee of the University of South Africa are thanked for financial assistance.

References

- Andrew E R and Canepa P C 1972 *J. Magn. Reson.* **7** 429
Jurga S, Jurga K and Pajak Z 1981 *J. Phys. C: Solid State Phys.* **14** 4433
Kozak A, Grottel M, Koziol A E and Pajak Z 1987 *J. Phys. C: Solid State Phys.* **20** 5433
Reynhardt E C and Lourens J A J 1984 *J. Chem. Phys.* **80** 6240
Smith S G 1959 *PhD Thesis* University of California at Los Angeles
Sutton L E (ed) *Tables of Interatomic Distances and Configuration in Molecules and Ions* 1958 (London: The Chemical Society)
Van Vleck J H 1948 *Phys. Rev.* **74** 1168
Watton A, Petch H E and Pintar M M 1970 *Can. J. Phys.* **48** 1081
Zakzhevskii V G, Boldyrev A I and Charkin O P 1980 *Chem. Phys. Lett.* **73** 54
Zimmermann I C, Barlow M and McCullough J D 1963 *Acta Crystallogr.* **16** 883